



Optimization of dry heat treatment of egg white in relation to foam and interfacial properties

E. Talansier^{a,*}, C. Loisel^a, D. Dellavalle^b, A. Desrumaux^a, V. Lechevalier^c, J. Legrand^d

^a GEPEA-ENITIAA-UMR-CNRS 6144, Nantes, France

^b LTN-UMR-CNRS 6602, Nantes, France

^c UMR 1253 STLO, Agrocampus Rennes, INRA, F-35000 Rennes, France

^d GEPEA-UMR-CNRS 6144, Université de Nantes-IUT de St-Nazaire, CRTT, St-Nazaire, France

ARTICLE INFO

Article history:

Received 25 March 2008

Received in revised form 4 September 2008

Accepted 16 September 2008

Keywords:

Dry-heating

Egg albumen powder

Interfacial films properties

Adsorption kinetics

Foam properties

ABSTRACT

The properties of foams processed with reconstituted egg white were investigated as a function of the denaturation undergone by the proteins during the pasteurization stage in dry state. Various time-temperature tables were applied on the original egg white powder, ranging from 1 to 7 days, and from 60 to 80 °C. Differential Scanning Calorimetry was used to determine the denaturation degree of each EWP induced by the dry heat treatment. The rheological properties of the interface, using the drop tensiometer method, were shown to be significantly affected by the denaturation and to be a relevant parameter for foamability, stability and foam texture. The bulk properties of the foams were interrelated with interfacial properties by using principal component analysis (PCA) and cluster analysis (HCA). The resulting classification of the heat treatments reveals that mild treatment offers a good compromise between the heating cost and the functional properties of the foams.

© 2008 Swiss Society of Food Science and Technology. Published by Elsevier Ltd. All rights reserved.

1. Backgrounds and objectives

Egg white is qualified as multi-purpose ingredient. It combines high nutritional qualities with excellent functional properties. Hence, egg white proteins (EWP) traditionally play the role of natural surfactants in many applications of the food industry.

This material can be commercialised under various forms, including liquid solutions, but the more frequently encountered is in pulverulent state obtained by spray drying. Pasteurization of EWP remains an essential step of the industrial process because of microbiological food safety purposes. For this reason, liquid egg white is heated up at 58 °C for a few minutes, whereas packaged powder is usually stored in drying kilns at 55–80 °C for few days.

As underlined by Lechevalier, Jeantet, Arhaliass, Legrand, and Nau (2007), each stage of the fresh white egg industrial process can influence the EWP solution quality. In particular, pasteurization is a critical point of the process, as far as the functional properties can be damaged. For these reasons, the influence of the pasteurization on the EWP functional properties has been widely studied, especially in the liquid phase.

For instance, Van der Plancken, Van Loey, and Hendrickx (2007a) studied the influence of heat and high pressure treatment on the foaming properties of native liquid egg white solutions. The foams elaborated from heated and pressurized EWP solutions exhibit creamy texture and improved stability compared to the untreated ones.

Purified fractions have also been studied. Pezennec, Gauthier, Alonso, Graner, Croguennec, and Brule (2000), and Renault, Pezennec, Gauthier, Vié, and Desbat (2002) developed a set of methods for interface rheological measurements for ovalbumin and s-ovalbumin. The interfacial properties of heated solutions of ovalbumin were also investigated by Croguennec, Renault, Beaufils, Dubois, and Pezennec (2007), whereas Lechevalier et al. (2005) studied the ovalbumin, ovotransferrin and lysozyme ternary mixture to gain a better understanding of the mechanisms involved by the proteins interactions at the air–water interface. The kinetics of adsorption as well as the rheology of the interfacial layer were shown to be markedly modified by the heat treatment.

Concerning dry heat treatments, Kato, Ibrahim, Watanabe, Honma, and Kobayashi (1989) showed a significant increase of EWP functionality (foaming, emulsifying and gelling properties) by heating egg white powders at 80 °C during various periods (0–9 days). Among previous studies on this topic, Matsudomi, Ishimura, and Kato (1991) demonstrated the improvement of gelling properties of purified ovalbumin solution by dry heat treatment. Matsudomi, Takahashi, and Miyata (2001) completed these results

* Corresponding author. GEPEA-ENITIAA-UMR-CNRS 6144, BP 82225, 44332 Nantes, France.

E-mail address: etalansier@gmail.com (E. Talansier).

more recently, with the study of some structural properties of similar solutions in order to clarify the mechanisms of gelling properties enhancement by the heat treatment. Van der Plancken, Van Loey, and Hendrickx (2007b) focused on the effect of moisture content of the powder samples, concluding that it is a key process parameter, as well as temperature or pH in EWP dry-heating process. Nonetheless, the usual method of dry state pasteurization is particularly costly in time and energy storage facilities. To compensate this problem, Hammershoj, Nording, Rasmussen, Carstens, and Pedersen (2006) investigated the feasibility of an alternative process by fluidized bed, and its microbiological and functional consequences on the proteins. They highlighted that within moderate time (<2 h), at high temperature (115–130 °C), and with high air moisture level, the effects on bacterial elimination, protein polymerization, surface hydrophobicity development were comparable to the effects obtained by traditional dry pasteurization.

Despite some attempts to explain the rheological behaviour of the foams by the bubble size distribution and the interfacial properties (Davis & Foegeding, 2007; Foegeding, Luck, & Davis, 2006; Pernell, Foegeding, Luck, & Davis, 2002), the connection between interfacial and macroscopic properties remains confused (Le Floch-Fouéré et al., 2009).

The objective of this work is to characterise the foams (foamability, stability and texture), firstly to correlate them with the EWP solutions properties (DSC profiles, dynamic surface tension, viscoelasticity of the interface), and secondly to examine the evolution of these parameters following the intensity of the thermal treatment.

2. Materials and methods

2.1. EWP heat treatment

Egg White Proteins (EWP) powder was supplied from the Igreca Company™ (Seiches sur le Loir 49, France) directly after spray drying. The protein content of EWP powder is of 78.7% (wet basis) including lysozyme.

The pasteurization treatment was performed in the laboratory, onto 1 kg batches of EWP powder packaged in plastic bags. In the oven (VC 7018, Vötsch Industrietechnik™, Germany), the relative moisture was monitored at 40%. The samples were submitted to different time–temperature tables, from 1 to 7 days and from 60 to 80 °C. The untreated powder is referred “NP” (No Pasteurization treatment), and the different heat treatments are referred x-y, x for the temperature and y for the number of days.

The EWP solutions are prepared by powder’s rehydration with tap water at room temperature at 12.5% (w/w) powder (i.e. 9.84% w/w of protein content). The complete dissolution is achieved in two steps: the powder is at first pre-mixed with 20% of the total water, till obtaining of a smooth and homogeneous paste, and then the remaining amount of water is added and the suspension gently stirred for 1 h. The pH was controlled and is set in the range of [7.3–7.6].

2.2. Physicochemical properties of EWP solutions

2.2.1. Thermal analyses

Differential Scanning Calorimetry (DSC) was used to assess the changes in proteins conformation induced by thermal denaturation (Harwalkar & Ma, 1996). DSC was performed using a microcalorimeter (SETARAM, micro DSC III, France). A volume of 800 µL of EWP solution is sealed in a hermetic stainless steel pan, and water is used in the reference cell. The heat-up ramp is from 20 to 100 °C at the rate of 0.5 °C/min. The ovalbumin peak denaturation temperature is taken as characteristic value of the denaturation degree, and the overall enthalpy of denaturation is calculated from 50 to 90 °C.

2.2.2. Surface tension measurements

The surface tension is measured using the pending drop method (Interfacial Technology Concept™, Longessaigne, France). An air bubble (8 µL) is formed at the tip of a capillary fitted to a syringe, whose piston is driven by a motor, into a thermostated optical glass bowl containing 15 mL of the EWP solution (12.5% (w/w) diluted at 1/100 in ultra pure water (i.e. 0.0984% w/w of protein content)). The image of the bubble is taken from a CCD camera and digitalized. As the actual shape of the drop results from the antagonistic effects between the interfacial tension and the gravity forces, the surface tension σ [Nm⁻¹] can be calculated by analysing the contour of the bubble according to the Laplace–Young equation. The most decisive drop parameters are the shape factor and the curvature radius at the apex. A complete description of the experimental set-up and analysis methods is given by Benjamins, Cagna, and Lucassen-Reynders (1996).

The surface tension measured as a function of time, also called “dynamic surface tension measurements”, results in the study of the adsorption kinetics of the surfactants. (Langevin, 2000). According to the literature (MacRitchie, 1990; Miller et al., 2000) proteins adsorption kinetics can be divided in three – or four – successive steps: (i) a lag period, (ii) the diffusion of the protein from the bulk onto the interface, (iii) the adsorption (penetration) and interfacial unfolding, and (iv) rearrangement within the interface layer, multilayer formation and interfacial gelation.

The lag period (step 1) is characterised by the plateau duration at σ_0 , namely τ_{lag} . In the second step, the diffusion of the proteins at the air–interface governs the adsorption process, and can be described by the equation:

$$\pi = 2C_0 \left(\frac{k_{diff}t}{3.14} \right)^{1/2} \quad (1)$$

where π represents the pressure surface, defined as $\sigma_0 - \sigma$ [mN m⁻¹], C_0 [wt%] the bulk protein concentration, t the current time and k_{diff} the diffusion rate. A plot of π against $t^{1/2}$ gives the k_{diff} constant (de Feijter & Benjamins, 1987; MacRitchie, 1978; Ward & Torday, 1946; Xu & Damodaran, 1994). To model both adsorption/penetration/unfolding (step 3) and later rearrangement/multilayer formation phenomena (step 4), the “first order law” approach proposed by Graham and Phillips (1979) can be used:

$$\ln \left(\frac{\pi_{final} - \pi_t}{\pi_{final} - \pi_0} \right) = -k_i t \quad (2)$$

where $k_i = k_{ads}$ or k_{rear} , depending on the considered phenomena. A plot of Eq. (2) usually yields two or more linear regions, giving in the first zone the constant rate of penetration k_{ads} , while the second slope corresponds to a constant rate of protein rearrangement k_{rear} . It was noticed that the rearrangement phase (step 4) begins at around 3000 s in our experiments. Hence, this last step will not be taken into account in this study as it exceeds our measurement time (3600 s).

The surface tension at 3600 s, $\sigma_{3600 s}$, is assumed to yield the equilibrium surface tension σ_{eq} .

The parameters τ_{lag} , k_{diff} , k_{ads} and σ_{eq} were retained as characteristic values of the EWP adsorptions kinetics at the air/solution interface. Table 1 lists the surface tension values depending on the heat treatment.

2.2.3. Interface viscoelasticity measurements

The oscillatory measurements of the bubble dilatation were performed after a released time of 1 h. Pulsations of the syringe were controlled by a stepping motor for application of a sinusoidal deformation of the drop surface within a few percent, in the linear domain, in the frequency range [0.005–0.05] Hz.

Table 1
Characteristic parameters

Heat treatment conditions	Standard deviation (%)	NP ^a	60–3	70–1	70–3	80–1	75–3	75–5	80–3	75–7	80–5
EWP solutions characterisation											
T [°C]	0.06	77.24a	77.21a	77.13b	76.92c	76.88c	76.72d	76.33e	76.17f	75.83g	75.67h
Enthalpy [J/g of proteins]	4	12.3a	12.4a	11.6b	11.5b	10.8c	10.7c	10.2d	8.9e	8.5e	7.9f
τ_{lag} [s] ^b		1.9	2.6	2.1	2.3	2.5	1.1	1.8	2.2	2.1	1.5
k_{diff} [mN m ⁻¹ s ^{-0.5}] ^b		3.27	3.14	3.44	2.79	3.13	2.82	2.85	2.18	2.66	2.75
$k_{\text{ads}} \times 10^4$ [s ⁻¹] ^b		10.0	9.0	10.3	9.9	9.3	10.3	9.9	9.5	9.1	8.0
σ_{eq} [mN m ⁻¹]	7	49.1a, b	49.3a, b	49.1a, b	49.5a	49.1a	48.6a, b, c	48.3a, b, c	47.6c	47.7b, c	47.8b, c
$ \epsilon^* $ [mN m ⁻¹]	3	67.6a	69.1b	67.8a	61.2c	52.4d	52.2d	47.0e	42.3f	44.7g	43.0h
Foams characterisation											
OV [%]	4	789a	905b	864c, d	859d	824e	863d	890b, c	858d	899b	892b
t_0 [s]	17	1475a	2037b, c	2124b, c	3077d	2073b, c	2490e	2276c, e	2082b, c	2188c	1963b
$\tau_{\text{retention}}$ [s] ^b		2684	2639	2686	4055	3871	4305	4174	4252	4329	4301
$ G^* $ [Pa]	8	3507a	3281b	3274b	2631c	1900d	2092d	2107d	1592e	1485e, f	1357f
D_M [μm]	7	95a	92a	83b	77c	79b, c	74c, d	70d, e	66e	66e	67e
Dispersion index [μm]	10	42a, b	46a	46a	44a	48a	45a	45a, b	39b	45a	44a

Values with different letters indicate Statistical significance.

^a NP: No Pasteurized powder, reference condition.

^b Values without index are averaged over a set of repeated runs.

The complex elasticity modulus $|\epsilon^*|$ at the frequency of 0.01 Hz, was retained as the characteristic parameter of the interface viscoelasticity measurements.

2.3. Physical properties of the EWP foams

2.3.1. Foaming method

Foams were processed by whipping at room temperature 200 mL of EWP solutions in a standard mixer KitchenAid (KSM90, USA) with rotating beaters at speed 10 (265 rpm planetary rotation with a beater rotation of 2.25 per planetary rotation) for 5 min.

2.3.2. Overrun

Directly after whipping, the foam produced was gently transferred into a preweighted flat Pyrex Petri dish (100 mL) using a stainless steel spatula. Excess foam was scraped from the top of the dish with a glass thin slide to level the upper surface.

The overrun was measured by weighing equal volumes of solution and foam, and calculated as follows:

$$\%OV = \frac{(\text{wt } 100\text{mL solution}) - (\text{wt } 100\text{mL foam})}{(\text{wt } 100\text{mL foam})} \quad (3)$$

2.3.3. Foam stability and liquid drainage

The same container is turned upside down and placed upon a balance. The weight of drained liquid was collected and recorded over 180 min.

2.3.3.1. Foam stability. The drainage of the interstitial liquid begins at the instant t_0 , estimated by the first drop impact. This parameter is considered as the characteristic of foam stability.

2.3.3.2. Liquid drainage. The cumulative weight of drained liquid $m_i(t)$ recorded after the lag time t_0 was used to characterise the gradual draining of the interstitial liquid foam. The cumulative weight is normalized by the initial weight of liquid in foam, $M_{\text{init},i}$ and measured over 10,800 s.

$$M_i(t) = \frac{m_i(t)}{M_{\text{init},i}} \quad (4)$$

Stability curves were fitted by a first order equation, where the t_0 value is taken from the average of the experimental

runs, and $\tau_{\text{retention}}$ is the characteristic time of the liquid drainage.

$$M(t) = \frac{1}{C} \left\{ 1 - \exp \left[- \frac{t - t_0}{\tau_{\text{retention}}} \right] \right\} \quad (5)$$

2.3.4. Rheological measurements

The rheological properties were measured by using a stress-controlled rheometer AR1000-N Rheolyst™ (TA Instruments, France), thermostated by Peltier effect, equipped with a parallel plate geometry of 40 mm diameter, with a gap of 2.5 mm. The foam sample was carefully loaded directly after whipping onto the lower plate of the rheometer. The measurements were performed in oscillatory mode, in the frequency sweep 0.1–10 Hz range, at 0.5% strain and 4 °C. The viscoelastic modulus $|G^*|$ at 1 Hz is retained as characteristic value.

2.3.5. Bubbles size distribution

Small samples of foam are placed onto a microscope slide, likewise directly after whipping. Pictures of foam bubbles (Fig. 1) were taken using a CCD camera mounted on a Leica™ microscope (Wild M3C, magnification 40) as quickly as possible.

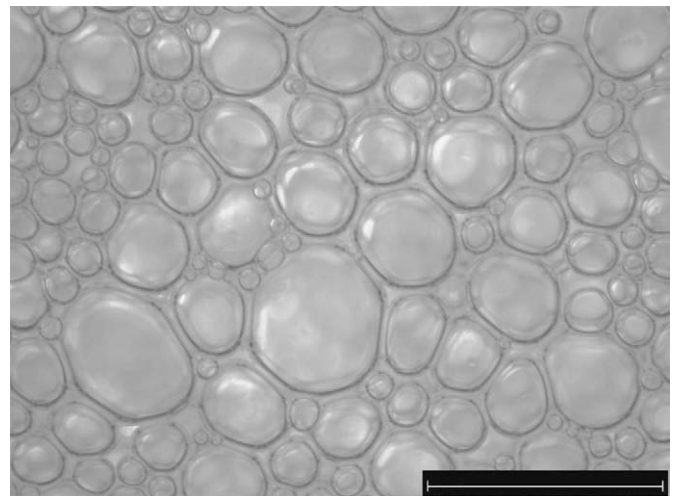


Fig. 1. Example of image acquired (75–7 heat treatment condition, bar scale = 500 μm).

Bubbles size and morphology were analysed with the image analysis software Visilog6.2™ (Noesis). A semi-automatic procedure was developed to estimate the bubble areas, unless a manual intervention remains necessary to avoid the incomplete contours. The equivalent diameter $d_i = \sqrt{4A/\pi}$ is computed with 5–20 images, *i.e.* 500–1200 bubbles for each treatment, as recommended for statistical purposes (Labbafi, Thakur, Vial, & Djelveh, 2007; Vigneau, Loisel, Devaux, & Cantoni, 2000).

The bubbles size distribution is fairly described by a log-normal law:

$$f(d) = \frac{1}{\sqrt{2\pi}\sigma} \frac{1}{d} \exp\left\{-\frac{1}{2}\left[\frac{\ln(d/m)}{\sigma}\right]^2\right\} \quad (6)$$

with m = mean ($\ln(d)$) and σ = standard deviation ($\ln(d)$) obtained from the diameter series. Bubbles populations were characterised by the modal diameter D_M and the dispersion index DI of the distribution, defined as:

$$\begin{aligned} D_M &= \exp[m] \quad [\mu\text{m}] \\ DI &= sh \quad \sigma \quad [\mu\text{m}]. \end{aligned} \quad (7)$$

2.4. Repeatability and statistical analysis

For both EWP solution and foam characterizations, the experimental repeatability conditions used for the determination of the parameters are reviewed in Table 2.

Using the One way ANOVA procedure of the StatgraphicsPlus5.0® software, significant differences were found between the different runs at the level of 5%.

To point out a potential correlation between interfacial properties of the solution and those of the foams, the set of characteristic variables was submitted to principal component analysis (PCA) of SPAD software (Decisia™, Pantin, France). Response variables which discriminated significantly between steps were analysed by cluster analysis (HCA).

3. Results

3.1. Influence of the heat treatment on the properties of the interfacial film of the EWP solutions

3.1.1. Thermal analysis

DSC is used to evaluate the denaturation undergone by the EWP powders due to the dry heat treatment. In addition, DSC profiles of fresh white egg show the partial denaturation induced by the spray-drying process before the pasteurization, when comparing the native and the NP material. The enthalpy peaks are 19.5 and 12.3 J/g for native and NP conditions, respectively, leading to an absolute denaturation degree of 37% for the NP proteins.

Typical egg white thermograms exhibit two main peaks, around 60 and 80 °C. The first one is due to denaturation of

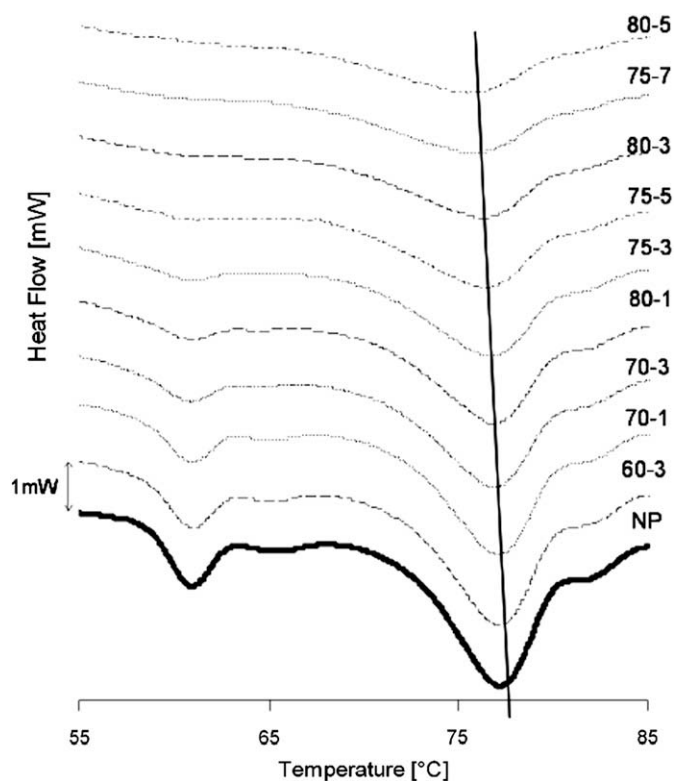


Fig. 2. Typical thermograms obtained with EWP solutions at 12.5% (w/w) for various thermal treatments. From bottom to top heat-treated conditions are: Native (NP), 60–3, 70–1, 70–3, 80–1, 75–3, 75–5, 80–3, 75–7, 80–5 conditions. The scale on the left represents 1 mW and the heating rate was carried out at 0.5 °C/min.

ovotransferrin and the second to the denaturation of ovalbumin. The small intermediate peak is due to the denaturation of lysozyme. This peak is less pronounced for the native egg white than for the NP powder, as seen in Fig. 2. These thermograms are similar to those obtained by Donovan, Mapes, Davis, and Garibaldi (1975). In their case, the three endothermic peaks appear at 65, 74 and 84 °C. In comparison, the values for the NP condition are 61, 65 and 77 °C. The use of a slower heating rate of denaturation – 0.5 °C/min in the present study, whereas Donovan's one is 10 °C/min – is responsible of these differences. In fact, and that is confirmed by our results, it is specified in the same study that slower heating rates leads to somewhat narrower peaks, occurring at lower temperatures.

As it is shown in Fig. 2, increasing the intensity of the heat treatment leads to a gradual broadening and a decrease of the peaks, as well as a shift of the peak temperature to lower values. The enthalpy values decrease from 12.3 to 7.9 J g⁻¹ when the ovalbumin peak is shifted from 77.2 to 75.7 °C (Table 1). For the highest heat treatment conditions, *e.g.* from 75–5 to 80–5, both ovotransferrin and lysozyme peaks tend to disappear while the ovalbumin peak is damped.

These results are in accordance with the literature (Kato, Ibrahim, Watanabe, Honma, & Kobayashi, 1990). These authors found a dramatic decrease of the denaturation enthalpy and a slight decrease in denaturation temperature that they ascribed to partial unfolding of the proteins due to heat treatment in the dry state.

3.1.2. Surface tension measurements

As previously stated, EWP adsorptions kinetics can be divided in four steps: the lag period, diffusion, adsorption and rearrangement (*cf.* § 2.2.). The Fig. 3 presents the kinetics of the surface tension for the 80–5 condition, where the denaturation is the highest.

Table 2
Repeatability of the experiments

	Number of experimental runs	Standard deviation (%)
EWP solution characterisation		
T [°C]	3–4	0.06
Enthalpy [J/g of proteins]	3–4	4
σ_{eq} [mN/m]	3–9	7
$ \epsilon^* $ [mN/m]	1–6	3
Foams characterisation		
OV [%]	3–11	4
$ G^* $ [Pa]	4–6	8
D_M [μm]	1–4	7
Dispersion index [μm]	1–4	10

3.1.2.1. The lag period. The lag time, τ_{lag} , is the time required for the monomers to significantly lower the surface tension by adsorption at the interface. It is usually associated with the molecular flexibility and hydrophobicity. The lag period was observed by [Beverung, Radke, and Blanch \(1999\)](#) on ovalbumin and β -casein, and by [Perez, Sanchez, Pilosof, and Patino \(2008\)](#) on hydroxy-propyl-methyl cellulose (HPMC). As reported by [Miller et al. \(2000\)](#) the presence/absence of the lag period essentially distinguishes the adsorption behaviour of proteins and surfactants: the lag time, also named induction time, only exists for the proteins. The duration of the lag period is reported to increase with the inverse of the bulk concentration: the very low values obtained in the present study show that the covering of the interface by the EW proteins is instantaneous with the bubble formation. This result can be explained by the rather high bulk protein concentration used in our study (about 0.1%) compared to the ones of the literature (0.01%).

3.1.2.2. EWP diffusion to the interface. According to Eq. (1), the diffusion phenomenon is driven by the protein concentration gradient between the interface and the bulk aqueous phase. The values of k_{diff} are reported in Table 1; a slight decrease is observed with the increase of the denaturation.

3.1.2.3. EWP adsorption/penetration at the air–water interface. Further (over ~ 10 s, Fig. 3), the predominant phenomenon is the adsorption, penetration, unfolding and rearrangements of the monomers at the interface. The values of k_{ads} are consistent with those of [Perez et al. \(2008\)](#), for hydroxy-propyl-methyl cellulose (HPMC). Table 1 shows that k_{ads} values tend to decrease with the intensity of the heat treatment, which is especially manifest up to the 75-7 condition.

3.1.2.4. Equilibrium surface tension. The trend for σ_{eq} is to decrease with the increase of the heat treatment, but without any clear significant differences, as shown by the statistical analyses, in Table 1.

3.1.3. Interface viscoelasticity measurements

It can be observed that $|\varepsilon^*|$ values decrease as the heat treatment becomes more intense, with a relative gap of 37% between the extreme conditions (Table 1). It can be concluded that the denaturation due to dry heat treatment significantly affects the viscoelastic properties of the interfacial film. The decrease of the dilatational modulus is gradual from the 60-3 to the 80-3 conditions, until reaching a plateau; a stronger heat treatment does not

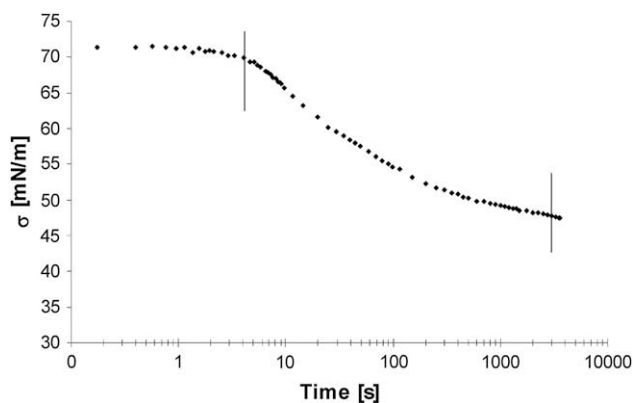


Fig. 3. The kinetics of EWP proteins at the air/liquid interface. Example given for the 80-5 condition. Experimental data evolutions – three successive steps are successively visible. First step: initiation (lag period) and diffusion. Second step: adsorption. Third step rearrangement.

modify the interfacial properties. This indicates that the rigidity of the interfacial film is reduced by the dry heat treatment.

3.2. Influence of the heat treatment on the physical properties of the EWP foams

3.2.1. Overrun

The overrun OV indicates the gas hold-up in the EWP foam. Experimental values measured for each heat treatment condition are reported in Table 1. The comparison between the overrun of heat-treated EWP and NP one shows a clear increase of the overrun values (about 12%). But no significant evolution can be detected between the nine denaturation levels. The volume fraction of the foams deduced from the overrun values is 0.88 and 0.90 for non-heated and heated EWP, respectively. This high volume fraction characterizes dry foams.

3.2.2. Foam stability and liquid drainage

The values of t_0 the first drop occurrence and $\tau_{\text{retention}}$ the characteristic drainage time are summarized in Table 1.

Globally, the stability of heat-treated products is improved compared with the NP one. This is a well-known beneficial effect of the heat treatment of EWP, as well in liquid phase ([Hagolle, Relkin, Popineau, & Bertrand, 2000](#)) as in the dry state ([Kato et al., 1990](#)). An optimum of stability is reached for 70-3, corresponding to the highest t_0 value. For higher treatment conditions, both t_0 and $\tau_{\text{retention}}$ remain unchanged.

3.2.3. Rheological measurements

All the foams exhibit solid-like behaviour as the storage modulus G' exceeds the viscous modulus G'' (3–7 times). Previous work by [Mleko, Kristinsson, Liang, and Gustaw \(2007\)](#) shows the same highly elastic behaviour but with values of the moduli which are tenfold lower than in our experiment.

As shown in Table 1, a decided decrease of the $|G^*|$ modulus arises for a higher degree of denaturation. These results clearly indicate a loss of texture resulting from the heat treatment that is perceptible by the change from brittle to softer texture of the foams.

3.2.4. Bubbles size distribution

The bubbles population is fully described by the modal diameter D_M and the dispersion index DI ; they are reported in Table 1 for each case. The modal diameter of the bubbles, 95 μm for unheated EWP is of the same order of magnitude than those found by [Van der Plancken et al. \(2007a\)](#), about 150 μm . Larger diameters are reported by [Hagolle et al. \(2000\)](#) probably due to the foaming process; whipping for the former, and sparging for the latter. The DI remains constant for all the samples.

In addition, it can be observed that D_M values are decreasing with the intensity of heat treatment. [Van der Plancken et al. \(2007a\)](#), who studied the effect of heat treatment up to 85–90 °C on EWP solutions (10% concentration, pH 7.6 of egg white solutions), reported the same observation.

3.3. Principal component (PCA) and cluster analyses (HCA)

The dependency of the foam and the liquid phase properties, especially through the interfacial ones, with respect to the denaturation conditions is investigated by PCA and HCA analyses. The first two principal components PC1 and PC2 explain a cumulative variation of 71.5%. The results are shown in Figs. 4, 5, and Table 3.

In Figs. 4 and 5, it can be seen that PC1 (58.8% of total inertia) sorts the runs according to the intensity of the treatment on the x-axis (lowest to highest intensity). Cluster analyses (HCA) identified three different groupings of the runs, underlined by the circles on Fig. 5:

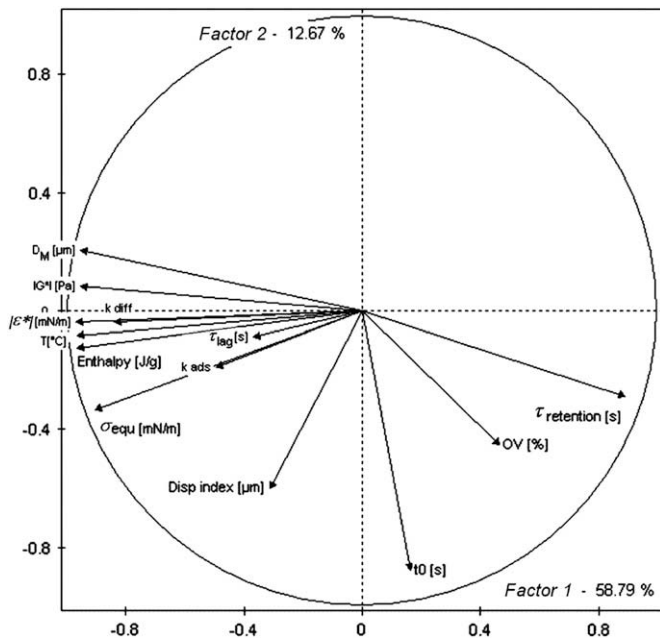


Fig. 4. Results of PCA analyses. Visualisation of PCA correlation according to PC2 vs. PC1.

low treated samples (NP, 60–3 and 70–1), mild treated samples (70–3, 75–3, 80–1 and 75–5) and high treated samples (75–7, 80–3 and 80–5). PC1 is correlated with DSC measurement (T^o and enthalpy, -97%), but also with surface tension measurements (k_{diff} , -84% ; k_{ads} , -84% ; σ_{eq} , -90%), interface viscoelasticity measurement ($|\epsilon^*|$, -97%), foam rheological measurement ($|\epsilon^*|$, -95%), foam bubble size (D_M , -95%) and foam stability ($\tau_{retention}$, $+89\%$).

On the y-axis, PC2 (12.7% of total inertia) discriminates the runs according to the stability of foams through the drainage lag time (time of the first drop occurrence t_0 , 88% , highest to lowest stability). Mild treatments (70–3) are opposite to both low and high heat treatment, so an optimum for mild treatments is underlined.

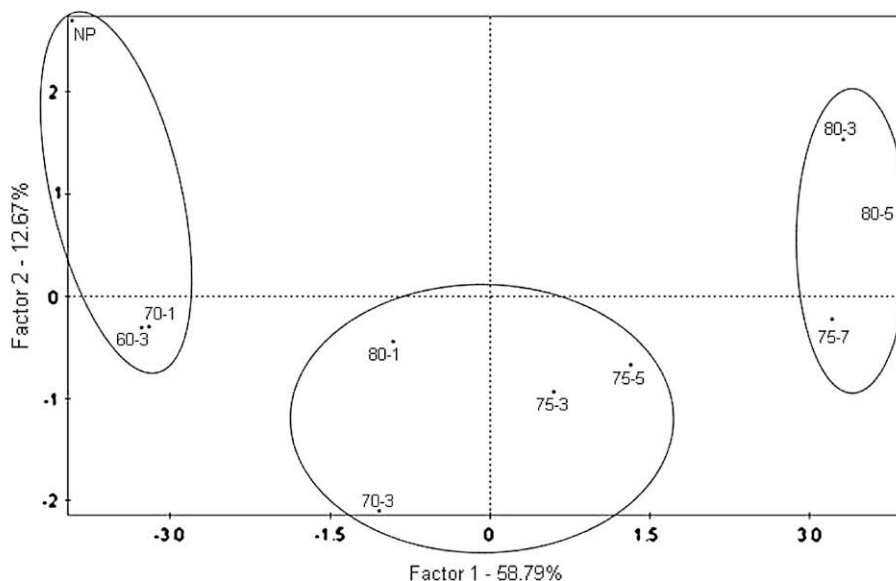


Fig. 5. Results of PCA analyses. Factorial map of the scores on the principal component 1 as a function of the scores on the principal component 2.

4. Discussion

In this work, the aim was to investigate the effects of the heat treatment in dry state on EWP powders, on the physicochemical properties of the EWP solutions, and in which extend they affect the functional properties of the corresponding elaborated foams. PCA and HCA analyses show that the level of the heat treatment provides a classification of the trials on PC1 projection axis. Three groups are identified, as function of the heat treatment intensity: low treated samples (NP, 60–3 and 70–1), mild treated samples (70–3, 75–3, 80–1 and 75–5) and high treated samples (75–7, 80–3 and 80–5).

DSC measurements are connected at 97% with the heat treatment on PC1. Indeed, the thermal characteristics of the EWP used in the present work, *i.e.* the denaturation enthalpy and the ovalbumin peak temperature clearly show a gradual decrease with the intensity of the treatment, which results in partial unfolding of the native structure. These results are in accordance with the literature, either concerning heat treatment carried out on solutions (Hagolle et al., 2000; Van der Plancken, Van Loey, & Hendrickx, 2006) or in terms of dry heat treatment (Kato et al., 1990). They proved that heat treatment produces irreversible conformational changes of the proteins in the dry state.

Considering the interfacial film, the denaturation produced by dry heat treatment results in the decrease of the parameters values, especially k_{ads} , showing a 60% correlation between T and k_{ads} coefficients (matrix of correlation, Table 3). These results are in agreement with Croguennec et al. (2007), who demonstrated that the heat treatment modifies the adsorption kinetics.

Moreover, dry heat treatment is also well correlated with the rigidity of the interfacial film (97% of correlation on PC1), showing a clear decrease of $|\epsilon^*|$ values with the increase of the heat treatment what clearly indicates a decrease in the rigidity of the interfacial film. This feature may be interpreted by the structure of the interfacial film that differs for heated EW proteins compared to unheated ones: as reported by Croguennec et al. (2007), the interfacial layer is less cohesive for heated solutions.

The concomitant decrease of the dilatational modulus and of the foam stiffness is confirmed by a 97% correlation coefficient between $|\epsilon^*|$ and $|G^*|$ values in the matrix (see Table 3). The similar evolution of these two rheological parameters is explained by the dry foam

Table 3
Results of PCA analyses – matrix of correlation

	C2	C3	C4	C5	C6	C7	C8	C9	C10	C11	C12	C13	C14
C2	1.00												
C3	0.98	1.00											
C4	0.36	0.34	1.00										
C5	0.72	0.72	0.16	1.00									
C6	0.60	0.58	-0.12	0.28	1.00								
C7	0.92	0.92	0.38	0.74	0.44	1.00							
C8	0.92	0.93	0.35	0.80	0.42	0.88	1.00						
C9	-0.50	-0.42	-0.04	-0.31	-0.43	-0.39	-0.32	1.00					
C10	-0.03	0.00	-0.01	-0.29	0.25	0.19	-0.09	0.33	1.00				
C11	-0.78	-0.78	-0.40	-0.79	-0.25	-0.65	-0.90	0.30	0.47	1.00			
C12	0.90	0.92	0.29	0.76	0.51	0.80	0.97	-0.35	-0.18	-0.91	1.00		
C13	0.89	0.90	0.34	0.79	0.30	0.81	0.93	-0.47	-0.36	-0.91	0.92	1.00	
C14	0.26	0.27	0.15	0.62	-0.03	0.45	0.26	0.20	0.17	-0.16	0.12	0.21	1.00

C2: T [°C]; C3: Enthalpy [J/g of proteins]; C4: τ_{lag} [s]; C5: k_{diff} [$\text{mN m}^{-1} \text{s}^{-0.5}$]; C6: $k_{\text{ads}} \times 10^4$ [s^{-1}]; C7: σ_{eq} [mN m^{-1}]; C8: $|\varepsilon^*|$ [mN m^{-1}]; C9: OV [%]; C10: t_0 [s]; C11: $\tau_{\text{retention}}$ [s]; C12: $|G^*|$ [Pa]; C13: D_M [μm]; C14: dispersion index DI [μm].

behaviour. In fact, the foam framework consists of thin films where interfacial forces prevail. The foams hence present a loss of texture as increasing the heat treatment (95% of correlation on PC1).

For higher degree of denaturation, the loss of texture is accompanied by the decrease of the bubble size (95% for the correlation coefficient for D_M and $|G^*|$ on PC1, and 92% for the correlation coefficient between $|G^*|$ and D_M). Moreover, the decrease of the macroscopic properties (bubbles size and texture) with the increase of the treatment also corresponds to a better ability to retain the liquid drainage (for instance, correlation of 91% between D_M and $\tau_{\text{retention}}$). In fact, this latter parameter is also highly connected with the heat treatment, as the correlation between PC1 and $\tau_{\text{retention}}$ reaches 89%.

Is it then possible to correlate the stability of the foam with the dilatational modulus and consequently the texture of the foam? Matrix of correlation does not show any convincing correlation between t_0 and $|G^*|$, but a very high correlation between $\tau_{\text{retention}}$ and $|G^*|$ (91%).

According to the literature, the mechanisms governing the stability are complex. The destabilization mainly occurs by two mechanisms: on the one hand the liquid drainage from the Plateau border, that leads to the breaking of the interfacial film, and the coalescence of the bubbles, and on the other hand the disproportionation resulting in the growth of larger bubbles at the expense of the smaller ones. Under the present conditions, only the drainage of the liquid due to gravitational force can be observed (91% of correlation between $\tau_{\text{retention}}$ and $|G^*|$, matrix of correlation). The viscoelasticity of the interfacial film may contribute to the protection of gas bubbles but its effect varies according to the proteins concerned. Croguennec et al. (2007) found that native β -lactoglobulin, developing higher viscoelasticity (higher shear elastic constant) than heat-treated ones has a lower ability to stabilize the foams. Davis and Foegeding (2007) observed that higher viscoelasticity was linked with a higher stability concerning whey protein isolate and EWP, whereas Dickinson, Ettelaie, Murray, and Du (2002) and Le Floch-Fouéré et al. (2009) did not exhibit any correlation between the interfacial rheology and the foam stability. Some other factors such as the kinetics of protein adsorption on the interfacial film may play a major role on the overall foam stability. It can be only suggested that heat treatment of EWP in the dry state may favour the formation of an interfacial layer whose mechanical properties enhances foam stability.

Concerning PC2 axis, the only correlation is attributed to the foam stability parameter t_0 . The value of the coefficient correlation on PC2 is 88%. This can provide a complementary classification in addition of PC1. That classification divides experimental denaturation conditions by opposing extreme treatment: lower (NP) and higher (80-3, 80-5) treatments form one group, and mild

treatments a second one. An optimum, 70-3 condition, is observed among the conditions forming that second group. From an industrial point of view, mild treatments (70-3, especially) are thus sufficient to optimize foam stability. It is interesting to note that these treatments correspond to average values for protein denaturation, interfacial film surface tension and viscoelasticity, foam bubble size and texture.

5. Conclusion

The dry heat treatment on EWP, in the range of 60–80 °C and 1–7 days, has been conducted using the same tables as in an industrial level. The denaturation of EWP was accurately assessed by calorimetry. Depending on the intensity of the treatment and consequently the level of denaturation, the functional properties of the foams, in particular the stability and the ability to prevent the drainage were improved. This positive effect on the functional properties is concomitant with a decrease of the interfacial film viscoelasticity and of the foam rigidity, as well as the reduction of the bubbles size.

The correlation between interfacial properties of the solution and macroscopic behaviour of the foam is demonstrated. Thus, conditions of the heat treatment can be classified and optimized. Among the considerate conditions the mild treatments appear to be sufficient.

The approach developed in the present study is providing a method for optimizing the pasteurization stage in the egg white powder treatment, which may be beneficial for time and energy costs.

Acknowledgements

Dr Alain Riaublanc from the Research Center INRA of Nantes (F) is thanked for fructuous discussion on EWP.

References

- Benjamins, J., Cagna, A., & Lucassen-Reynders, E. H. (1996). Viscoelastic properties of triacylglycerol/water interfaces covered by proteins. *Colloids and Surfaces A: Physicochemical and Engineering Aspects*, 114, 245–254.
- Beverung, C. J., Radke, C. J., & Blanch, H. W. (1999). Protein adsorption at the oil/water interface: characterization of adsorption kinetics by dynamic interfacial tension measurements. *Biophysical Chemistry*, 81(1), 59–80.
- Croguennec, T., Renault, A., Beaufils, S., Dubois, J.-J., & Pezennec, S. (2007). Interfacial properties of heat-treated ovalbumin. *Journal of Colloid and Interface Science*, 315(2), 627–636.
- Davis, J. P., & Foegeding, E. A. (2007). Comparisons of the foaming and interfacial properties of whey protein isolate and egg white proteins. *Colloids and Surfaces B: Biointerfaces*, 54(2), 200–210.

- De Feijter, J. A., & Benjamins, J. (1987). Adsorption kinetics of proteins at the air–water interface. In E. Dickinson (Ed.), *Food emulsions and foams* (pp. 72–85). London, UK: Royal Society of Chemistry.
- Dickinson, E., Ettelaie, R., Murray, B. S., & Du, Z. (2002). Kinetics of disproportionation of air bubbles beneath a planar air–water interface stabilized by food proteins. *Journal of Colloid and Interface Science*, 252(1), 202–213.
- Donovan, J. W., Mapes, C. J., Davis, J. G., & Garibaldi, J. A. (1975). A differential scanning calorimetric study of the stability of egg white to heat denaturation. *Journal of the Science of Food and Agriculture*, 26, 73–83.
- Foegeding, E. A., Luck, P. J., & Davis, J. P. (2006). Factors determining the physical properties of protein foams. *Food Hydrocolloids*, 20, 284–292.
- Graham, D. E., & Phillips, M. C. (1979). Proteins at liquid interfaces. I. Kinetics of adsorption and surface denaturation. *Journal of Colloids and Interface Science*, 70, 403–414.
- Hagolle, N., Relkin, P., Popineau, Y., & Bertrand, D. (2000). Study of the stability of egg white protein-based foams: effect of heating protein solution. *Journal of the Science of Food and Agriculture*, 80, 1245–1252.
- Hammershoj, M., Nording, J. A., Rasmussen, H. C., Carstens, J. H., & Pedersen, H. (2006). Dry-pasteurization of egg albumen powder in fluidized bed. I. Effect on microbiology, physical and chemical parameters. *International Journal of Food Science and Technology*, 41, 249–261.
- Harwalkar, V. R., & Ma, C.-Y. (1996). Thermal analysis: principles and applications. In S. Nakai, & H. M. Modler (Eds.), *Food proteins: Properties and characterization* (pp. 405). New York, USA: VCH Publishers.
- Kato, A., Ibrahim, H. R., Watanabe, H., Honma, K., & Kobayashi, K. (1989). New approach to improve the gelling and surface functional properties of dried egg white by heating in dry state. *Journal of Agricultural and Food Chemistry*, 37, 433–437.
- Kato, A., Ibrahim, H. R., Watanabe, H., Honma, K., & Kobayashi, K. (1990). Enthalpy of denaturation and surface functional properties of heated egg white proteins in the dry state. *Journal of Food Science*, 55, 1280–1283.
- Labbafi, M., Thakur, R. K., Vial, C., & Djelveh, G. (2007). Development of an on-line optical method for assessment of the bubble size and morphology in aerated food products. *Food Chemistry*, 102, 454–465.
- Langevin, D. (2000). Influence of interfacial rheology on foam and emulsion properties. *Advances in Colloid and Interface Science*, 88(1–2), 209–222.
- Le Floch-Fouéré, C., Pezennec, S., Lechevalier, V., Beaufils, S., Desbat, B., Pérolet, M., et al (2009). Synergy between ovalbumin and lysozyme leads to non-additive interfacial and foaming properties of mixtures. *Food hydrocolloids*, 23(2), 352–365. Available online 11 February 2008.
- Lechevalier, V., Croguennec, T., Pezennec, S., Guérin-Dubiard, C., Pasco, M., & Nau, F. (2005). Evidence for synergy in the denaturation at the air–water interface of ovalbumin, ovotransferrin and lysozyme in ternary mixture. *Food Chemistry*, 92(1), 79–87.
- Lechevalier, V., Jeantet, R., Arhaliass, A., Legrand, J., & Nau, F. (2007). Egg white drying: influence of industrial processing steps on protein structure and functionalities. *Journal of Food Engineering*, 83(3), 404–413.
- MacRitchie, F. (1978). Proteins at interfaces. *Advances in Protein Chemistry*, 32, 283–326.
- MacRitchie, F. (1990). *Chemistry at interfaces*. San Diego, CA: Academic Press.
- Matsudomi, N., Ishimura, Y., & Kato, A. (1991). Improvement of gelling properties of ovalbumin by heating in dry state. *Agricultural and Biological Chemistry*, 55(3), 879–881.
- Matsudomi, N., Takahashi, H., & Miyata, T. (2001). Some structural properties of ovalbumin heated at 80 °C in the dry state. *Food Research International*, 34, 229–235.
- Miller, R., Faineman, V. B., Makievski, A. V., Krägel, J., Grigoriev, D. O., Kazakov, V. N., et al. (2000). Dynamics of protein and mixed protein/surfactant adsorption layers at the water/fluid interface. *Advances in Colloid and Interface Science*, 86, 39–82.
- Mleko, S., Kristinsson, H. G., Liang, Y., & Gustaw, W. (2007). Rheological properties of foams generated from egg albumin after pH treatment. *LWT - Food Science and Technology*, 40(5), 908–914.
- Perez, O. E., Sanchez, C. C., Pilosof, A. M. R., & Patino, J. M. R. (2008). Dynamics of adsorption of hydroxypropyl methylcellulose at the air–water interface. *Food Hydrocolloids*, 22(3), 387–402.
- Pernell, C. W., Foegeding, E. A., Luck, P. J., & Davis, J. P. (2002). Properties of whey and egg white protein foams. *Colloids and Surfaces A: Physicochemical and Engineering Aspects*, 204, 9–21.
- Pezennec, S., Gauthier, F., Alonso, C., Graner, F., Croguennec, T., & Brule, G. (2000). The protein net electric charge determines the surface rheological properties of ovalbumin adsorbed at the air–water interface. *Food Hydrocolloids*, 14(5), 463–472.
- Renault, A., Pezennec, S., Gauthier, F., Vié, V., & Desbat, B. (2002). Surface rheological properties of native and s-ovalbumin are correlated with the development of an intermolecular beta-sheet network at the air–water interface. *Langmuir*, 18, 6887–6895.
- Van der Plancken, I., Van Loey, A., & Hendrickx, M. E. (2006). Effect of heat-treatment on the physico-chemical properties of egg white proteins: a kinetic study. *Journal of Food Engineering*, 75(3), 316–326.
- Van der Plancken, I., Van Loey, A., & Hendrickx, M. E. (2007a). Foaming properties of egg white proteins affected by heat or high pressure treatment. *Journal of Food Engineering*, 78(4), 1410–1426.
- Van der Plancken, I., Van Loey, A., & Hendrickx, M. E. (2007b). Effect of moisture content during dry-heating on selected physicochemical and functional properties of dried egg white. *Journal of Agricultural and Food Chemistry*, 55, 135–137.
- Vigneau, E., Loisel, C., Devaux, M. F., & Cantoni, P. (2000). Number of particles for the determination of size distribution from microscopic images. *Powder Technology*, 107, 243–250.
- Ward, A. F., & Torday, L. (1946). Time dependence of boundary tensions of solutions. I: the role of diffusion in time effects. *Journal of Chemical Physics*, 14(7), 453–461.
- Xu, S., & Damodaran, S. (1994). Kinetics of adsorption of protein at the air–water interface from a binary mixture. *Langmuir*, 10, 472–480.